

Stable information transfer network facilitates the emergence of collective behavior in bird flocks

Jiaping Ren,¹ Wanxuan Sun,¹ Dinesh Manocha,² Aming Li,^{3,4} and Xiaogang Jin¹

¹*State Key Lab of CAD&CG, Zhejiang University, Hangzhou 310058, China*

²*Department of Computer Science and Electrical and Computer Engineering,
University of Maryland, College Park, MD, USA*

³*Department of Zoology and Oxford Centre for Integrative Systems Biology, University of Oxford, Oxford OX1 3PS, UK*

⁴*Chair of Systems Design, ETH Zürich, Weinbergstrasse 56/58, Zürich CH-8092, Switzerland*

(Dated: October 29, 2018)

Collective behavior is ubiquitous in living systems such as human crowds, microbial communities, insect swarms, and bird flocks. It is widely reported that simple, local, temporal interactions between individuals may lead to the emergence of collective behavior. In large-scale flocks, however, the global information transfer in dynamical models with time-varying neighborhoods is not normally instantaneous. Here, we present an information transfer network in which interactions last for a certain period of time. We then combine this network with a dynamic model of self-propelled particles. We observe that the resulting model that uses a stable information transfer network creates a bird flock with a more robust performance. We further show that the time of information transfer in a flock grows logarithmically with its size and is proportional to the average response time of the birds. Moreover, we find that the ranking curves displaying the order in which birds first perceive an external stimulus have similar shapes across different flocks. Our results demonstrate that, beyond the traditional local, temporal interactions, our stable information transfer network serves as an efficient mechanism to model the emergence of large-scale collective behavior.

I. INTRODUCTION

Collective behavior and cooperation of individuals in large groups are widespread in nature and occur in various species such as bacteria, midges, fish, birds, human beings, etc. [1–13]. Various theories of collective behavior have been developed in many fields, including ecology [14], biology [15, 16], physics [17–19], computer science [20], economics [21], control theory [22], and social science [23, 24]. As a unit, an aggregation often outperforms a simple sum of individuals [25]. For example, bird flocks escape from predators with a higher probability of success, honey bee swarms can find or build a comb, and bacteria colonies reverse their directions to expand rapidly [26–28]. One challenge is to figure out how do animals coordinate with each other to generate such adaptive collective behaviors.

With simple rules for local interactions, many collective behaviors among groups can be modeled [29, 30]. Many scientists are interested in a mechanism to produce global information transfer through local interactions. Marginal opacity was introduced to represent long-range information exchange [31]. Recently, scientists have come to believe that an individual bird interacts with six or seven birds on average, replacing the belief that a bird interacts with all other birds within a certain Euclidean distance [10, 32]. These models and empirical observations presume that birds interact with the birds nearest to them, which means that the neighborhood of each bird varies over time. However, the Coherent Neighbor Invariance theory states that the relationships among nearest individuals tend to be invariant in coherent behaviors [33]. In addition, it has been shown that equilibrium inference with a fixed interaction network can produce

consistent results with dynamical inference by analyzing the data from flocking events with 50 to 600 individuals [34]. Therefore, the fundamental mechanism that can explain the emergence of collective behavior in bird flocks is not well understood.

In this work, we use graph theory [35] to model the information transfer network of bird flocks. Within this stable information transfer network, each bird only transfers information with fixed neighbors and information received by one bird can be transferred to an arbitrary bird in the same flock. We further show that the time of information transfer in a flock grows logarithmically with its size. Moreover, we find that the ranking curves displaying the order in which birds first perceive an external stimulus have similar shapes for different flocks. Our experiments demonstrate that stable local interactions lead to more realistic and robust collective behavior, especially for large-scale flocks.

II. STABLE INFORMATION TRANSFER NETWORK: AN INVARIANT GRAPH

We construct a directed graph $G = (V, E)$ (Fig. 1A) to model the stable information transfer network of a bird flock, where V and E represent the sets of nodes and edges, respectively. We take the bird i in the flock as node $i \in V$ in G and define Ω_i as the set of nodes representing birds that have connections with node i . The number of nodes in V is N . E_i denotes the set of directed edges ending at i and starting from i 's neighbors, i.e. $E_i = \{e_{ji} | j \in \Omega_i\}$. The indegree of each node i is $d_{\text{in}}(i) = 6$, i.e. each bird only connects with six birds. Within this information transfer network, birds only per-

ceive information from the neighbors connected to them.

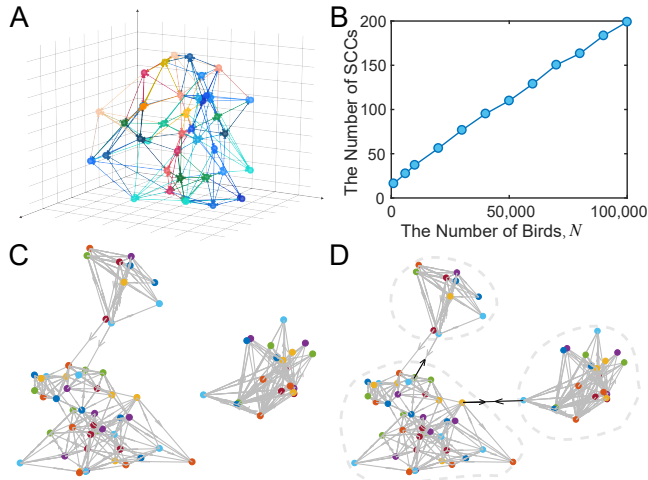


FIG. 1. (A) The invariant directed graph. Each node represents a bird in the flock and is adjacent to the six edges in the graph. If there are two arrows on one edge, the two nodes adjacent to this edge can propagate information with each other. (B) The number of strongly connected components increases (SCCs) linearly with the numbers of birds in a flock (the number of birds ranges from 1000 to 100,000). The nodes in each SCC can transfer information. We average the results of 10 different simulations. (C) The graph G describes the connections between birds (with 70 birds in total). For illustration, G contains three typical kinds of SCCs: sink, source, and isolated component, and each kind only has one sample. (D) We compute the strongly connected components of the graph shown in (C). Each component is distinguished from the others with a closed, dashed gray circle. We further add a minimum number of edges (black arrows) to make G strongly connected without changing the other edges.

We randomly assign node i in graph G a 3D position and find the six nearest nodes, which are designated as its neighbors. With the development of the whole flock's locomotion, these neighbors are not always the nearest neighbors. To explore the strong connectivity of G , we use the Eswaran-Tarjan algorithm [35] to find all the strongly connected components (SCCs) in which every node is reachable from other nodes. G is a strongly connected graph if it only has one SCC. In our experiments, we test flocks of 1000 to 100,000 birds. The number of strongly connected components corresponding to the number of birds in one flock is shown in Fig. 1B. With more birds, the number of strongly connected components of G is larger and G is farther from being a strongly connected graph. This indicates that information first obtained by a certain bird may not be propagated to all the other birds in the same flock; this is not consistent with the scale-free spatial correlation theory [36]. In addition, the birds that are not fully connected to other birds cannot receive useful information, such as danger signals in time to react. As a result, a strongly connected graph is needed to model the information transfer between the birds.

Taking the set of nodes V as input, we first add edges e_{ji} to connect each node i with its six nearest neighbors $j \in \Omega_i$ and then add edges to make G (Fig. 1C) strongly connected. To simplify the graph G , we find strongly connected components (SCCs) for G , condense G to a directed acyclic graph G^* , and then compute sources (with indegree zero), sinks (with outdegree zero), and isolated nodes (with both indegree and outdegree zero) of G^* (Fig. 1D). The nodes of G^* correspond to the strongly connected components of G .

Let s_1, s_2, \dots, s_p be sources in G^* and w_1, w_2, \dots, w_p be sinks, where p is the smaller number of nodes between the sources and sinks. Moreover, there exists at least one path p_i from s_i to w_i for $1 \leq i \leq p$. We add edges along the reverse path p'_i ($1 \leq i \leq p$); these edges share the same nodes but run in the direction opposite direction to p_i if and only if two adjacent nodes on the path p'_i are not connected. For all the nodes except for $s_i, w_i, i = 1, 2, \dots, p$ in G^* , we can add a reverse edge to the existing edge if the node is a source or a sink. If the node is an isolated node, we find the node nearest to it and add two edges with directions opposite to each other. Now that we have added edges to G^* , we move from adding the edges between two SCCs in G^* to adding the edges between two nodes in G , and then add the edges directly without changing other edges (Fig. 1D).

III. INFORMATION TRANSFER ON THE GRAPH

Information propagates along the strongly connected graph and each bird in the flock can perceive information from its neighbors. We use matrix A with entries 0 and 1 to represent the connection between birds, where $A_{ij} = 1$ means that bird i can perceive information from bird j and vice versa. Birds require a response time τ to sense the information. To simulate this phenomenon, we use the accumulated time to count the time elapsed during a response period. We first set the response time τ as a constant. The accumulated time \mathbf{T}_{j+1} of all birds at frame $j+1$ is generated from $\mathbf{T}_j = (T_{j,1}, T_{j,2}, \dots, T_{j,N})^T$, $\tau > T_{j,i} \geq 0$, and $T_{j+1,i} = H(\tau - T_{j,i} - \Delta t)(T_{j,i} + \Delta t)$, where the Heaviside function $H(x) = 0$ for $x < 0$ and 1 otherwise. As a result,

$$\mathbf{T}_{j+1} = \text{diag}(H(\mathbf{1}\tau - \mathbf{T}_j - \mathbf{1}\Delta t))(\mathbf{T}_j + \mathbf{1}\Delta t), \quad (1)$$

where Δt is the time unit, $\text{diag}(\mathbf{X})$ indicates where the main diagonal equals the vector \mathbf{X} , and $\mathbf{1} = (1, 1, \dots, 1)^T$.

The state of an external stimulus that affects the behavior of the flock may change over time. We use $s_j \in \mathbb{N}$ to represent the state ID of the external stimulus at frame j , where $s_{j+1} = s_j + 1$ and $s_0 = 1$. Due to the delay of information transfer, the state of each bird's perception of the external stimulus may be different at the same time instance. We use the vector $\mathbf{S}_j = (S_{j,1}, S_{j,2}, \dots, S_{j,N})^T$

to represent the information state IDs of the external stimuli that birds perceive at frame j . Each bird in the flock senses the external information from its neighbors at every τ time unit. A bird updates its current information state according to the newest information. The information state \mathbf{S}_{j+1} at frame $j+1$ can be updated from \mathbf{T}_j and \mathbf{S}_j (Eq. 2).

$$\mathbf{S}_{j+1} = \text{diag}(\mathbf{H}(\mathbf{T}_j + \mathbf{1}\Delta t - \tau))(B_1, \dots, B_i, \dots, B_N)^T, \quad (2)$$

where $B_i = \|\text{diag}(\mathbf{A}_i)\mathbf{S}_j\|_\infty$, \mathbf{A}_i is the i th row of \mathbf{A} and the initial state of $\mathbf{S}_0 = (0, 0, \dots, 0)^T$. When an external stimulus appears around the flock, n_r birds that are nearest to this stimulus will perceive it first. For simplification, we call n_r a reaction number. The information state \mathbf{S}_j corresponding to these n_r birds denotes as s_j .

A. Information transfer time

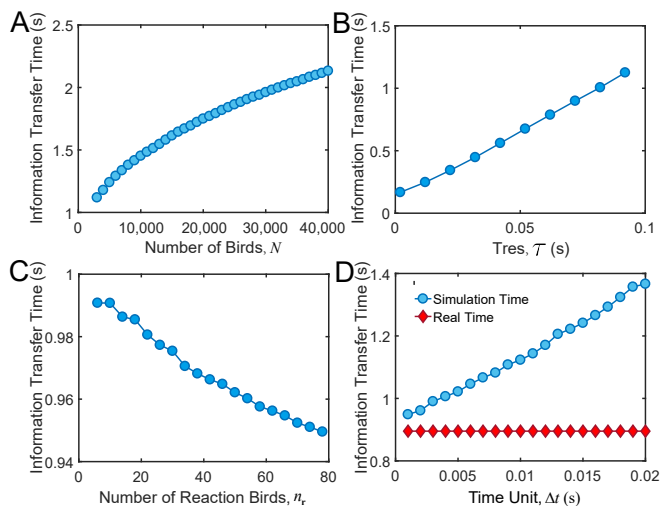


FIG. 2. The analysis of information transfer time. We obtain the following results by averaging over 10 simulations. (A) The information transfer time with different numbers of birds in one flock with the number of birds n ranging from 4,000 to 40,000, response time $\tau = 0.04s$, reaction number $n_r = 40$, and time unit $\Delta t = 0.01s$. (B) The information transfer time with different response times τ of birds, $N = 4,000$, $n_r = 40$, and $\Delta t = 0.01s$. (C) The information transfer time with different numbers of reaction birds, $\tau = 0.04s$, $N = 4,000$, and $\Delta t = 0.01s$. (D) The information transfer time with different time units, $\tau = 0.04s$, $n_r = 40$, and $N = 4,000$. The blue curve represents the information transfer time in the simulation and the red curve represents the estimation of the real information transfer time in which the simulation error is eliminated.

We define the longest directed path for information propagation starting from one of the n_r birds as l . The information transfer time Q refers to the time when $S_{j,i} \neq 0$, for all $i = 1, 2, \dots, N$ and

$$Q = l\tau. \quad (3)$$

For simulation, the information transfer time could be

$$T = l \left\lceil \frac{\tau}{\Delta t} \right\rceil \Delta t, \quad (4)$$

where $\tau \geq \Delta t$.

According to Eqs. (1) to (4), we choose the number of birds N , the response time of birds τ , the reaction number n_r , and the time unit Δt as the main influencing factors for the information transfer time Q of the flock. The simulation results are shown in Fig. 2.

The information transfer simulation time T grows logarithmically with the number of birds N in the flock (Fig. 2A). Because the information transfers through the graph with linear speed, the number of nodes perceiving the information increases exponentially. As a result, the depth of information transfer in the graph is linearly related to $\log(N)$. In other words, $l \propto \log(N)$ and thus $Q \propto \log(N)$, according to Eq. 3. The information transfer simulation time T is proportional to the response time τ (Fig. 2B). This simulation result agrees with Eq. 3, which shows $Q \propto \tau$.

The information transfer simulation time T is inversely proportional to the number of reaction birds n_r , but the decline of T is only approximately 3.7% when moving from 6 to 78 reaction birds, according to Fig. 2C. To estimate the theoretical time saved with an arbitrary n_r compared to $n_r = 1$, we can compute the information transfer time from 1 bird to n_r birds. Ideally, the information transfer time is $Q = \log_6(\frac{N}{n_r})\tau$. Thus, the transfer time saved using 78 birds compared to 6 birds could be 0.036s ($\tau = 0.04s$, '6' is the ideal number of neighbors for each bird). The fluctuation of Q in Fig. 2C mainly results from the randomness of the structure of graph G in each simulation.

The information transfer simulation time T is proportional to Δt , according to Fig. 2D. However, according to Eq. 3, Q should be irrelevant to Δt given that Q is only relevant to l and τ . This may result from the simulation error e which denotes the error caused by the simulation. According to Eq. 4, the range of error e could be $e \in [0, l\Delta t]$. We set $e = k\Delta t$ (k is a constant value) and obtain an estimate of the information transfer time, $\tilde{T} = T - k\Delta t$. As shown in Fig. 2D, the estimation of \tilde{T} is irrelevant to Δt , and this result is consistent with Eq. 3.

B. The process of information transfer through the flock

We simulate the information propagation through the bird flock and rank all birds in the flock according to the moment when they first become aware of the external stimulus. To verify the accuracy of our method, we also compare our results with the empirical observations from Attanasi et al. [37].

Up to this point, we have discussed information transfer time with the hypothesis that the birds' response time

is constant. In the real world, however, the response times cannot be the same for all birds, even if they are under the same physical conditions. We compare the ranked orders during an information transfer process in which τ is a constant and it follows a Gaussian distribution, which results in $\tau \sim N(\mu, \sigma^2)$. We set a minimum value for τ with Gaussian distribution because τ cannot be a negative value.

If τ is a constant, more birds are perceiving the external information at the same time and the ranking curve is continuous with τ being a Gaussian distribution (Fig. 3A). We find that the ranking curve of the flock with τ obeying a Gaussian distribution is closer to the real-world scenario, according to the empirical observations.

An information transfer network with a stable connection is easy to control; we only need to set parameters for the distribution of τ , including the mean μ , the standard deviation σ , and the minimum value of τ to generate various results (Fig. 3B). Meanwhile, our model captures the characteristics of the ranked birds in a flock, which are consistent with the empirical observations.

We also test our method with different sizes of flocks as shown in Figs. 3C and D, which display small flocks and large flocks, respectively. Further, these ranking curves are similar in shape, which indicates that the number of birds that sense the information increases slowly, then rapidly, and finally slowly again. The number of birds that perceive information $n(t)$ increases exponentially at first, which meets the ideal estimation that $n(t) = n_r 6^{\frac{t}{\tau}}$. Because of the fixed flock size N in one simulation, the change in $n(t)$ finally decreases.

IV. STABLE INFORMATION TRANSFER NETWORK VS. UNSTABLE INFORMATION TRANSFER NETWORK

Traditional methods assume that individuals interact with the nearest individuals within a certain Euclidean distance [29, 38, 39]. Recently, scientists discovered that a bird interacts with six or seven birds on average [10, 32]. By combining these advanced works, we compare our stable information transfer network with an unstable information transfer network in which each bird considers the six nearest birds. The stable information transfer network is static, while the unstable one is temporal. In this section, we compare the properties of these two networks.

A. Self-propelled model

Groups of individuals adjust their velocities according to those of their local neighbors and external stimuli. In existing particle-based models [29, 31, 38], local interactions occur only among the nearest agents. Instead, we

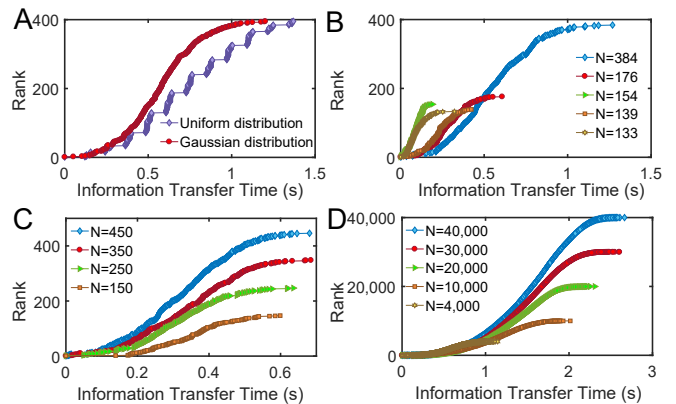


FIG. 3. The process of information transfer through the flock described by the ranking curve of birds sorted by the time at which they first perceive information. (A) Comparison of different methods for generating response time τ for birds: constant (the purple curve) and Gaussian distribution (the red curve) of different birds. τ is invariant for one bird with a Gaussian distribution. (B) Simulation results with different sizes of flocks for comparison with real datasets [37]. (C) Simulation results with a small number of birds in one flock; the number of birds ranges from 150 to 450. These results use the same parameter values: the distribution of τ , the reaction number of birds n_r , and the time unit Δt . (D) Simulation results with a large number of birds in one flock, with the number of birds ranging from 4,000 to 40,000. They also use the same parameters.

believe that individuals in a group mainly have local interactions with fixed sets of individuals. We use cohesion force, alignment force and repulsion force to describe the effects of local interactions among birds based on the interaction rules in Ref. [38] (see the Appendix for more details). In contrast to the existing particle-based models, cohesion force and alignment force only occur among agents that have connections with each other, while repulsion force occurs among individuals within a certain distance for collision avoidance.

B. Comparison

With our self-propelled model, we can simulate the common behavior of bird flocks avoiding a predator. By analyzing ranking curve, polarization $\Phi_j = \left\| \frac{1}{N} \sum_{i=1}^N \frac{v_{i,j}}{\|v_{i,j}\|} \right\|$ (which measures the overall degree of alignment), and spatial correlations $C(r)$ (which measures the behavior correlation among birds in a distance range $d \in [r-1, r]$) (see the Appendix for more details). We compare the stable information transfer networks and unstable information transfer networks with empirical observations [36, 37].

The ranking curve of the stable information transfer network is an S-curve while that of an unstable information transfer network is an exponential curve (Fig. 4A). This is because, for an unstable information transfer net-

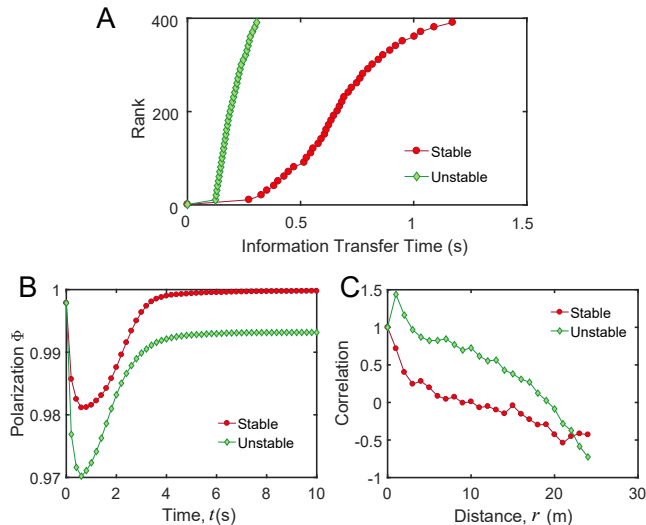


FIG. 4. Comparison between the stable information transfer network (the red curve) and the unstable one (the green curve). (A) The rank of each bird in an information transfer sequence is plotted against the time when it perceives the information. (B) Polarization as a function of time in stable or unstable information transfer networks. The time is counted from the start of the transfer of information about an external stimulus. (C) This correlation function measures the correlation of the orientation of velocity fluctuations among birds in a certain distance range. It is the average inner production of the velocity fluctuations of bird pairs at a mutual distance r .

work, a bird will move towards the flock once it senses danger and transfer that information to birds that are far from it. The ranking curve for the stable information transfer network is closer to that of the empirical observations [37].

Polarization is a quantity that describes the coherence of the flock. If $\Phi_j = 0$, the directions taken by the birds in this flock are totally random while if $\Phi_j = 1$, all birds in this flock move in the same direction. The polarization for a stable information transfer network is larger than that for an unstable information transfer network (Fig. 4B). This shows that the behaviors of birds in the flock with a stable information transfer network are more consistent when they confront a predator.

The spatial correlation of fluctuation (see the Appendix for details) is plotted in Fig. 4C. The spatial correlation of the flock with a stable information transfer network is close to 1 at short distances, decays dramatically with a gradually decreasing rate as the distance increases, and tends to be negative at large distances. Although the spatial correlation with an unstable information transfer network decays dramatically at short distances, it decays with an approximately constant rate as the distance increases. The spatial correlation for a stable information transfer network is closer to the real-world one [36].

We visually compare simulation results of the stable information transfer network with those of the unstable information transfer network (see Supplemental Material Movies S1-S2 [40]). We separately test these two methods with

a fixed danger stimulus and a moving danger stimulus. Birds simulated by our method remain cohesive over time, while birds tend to separate with the unstable information transfer network. The cohesion of the bird flock when it encounters a predator is affected by the structure of the information transfer network due to the attraction of birds in the neighborhood. If the information transfer network is strongly connected, the birds will always fly together no matter how often the structure of the information transfer network is updated. If the information transfer network is not strongly connected, the birds will always fly together if they are in the same strongly connected component so that the global cohesion is indistinctive, regardless of changes to the update frequency of the information transfer network.

The information transfer time Q depends on the update frequency of the information transfer network f , the response time of the birds τ , the average minimal distance among neighbors d_{\min} , and the average velocity difference in the desired direction between two neighbors Δv . If $\tau \leq d_{\min}/\Delta v$, Q will not change dramatically when f increases. Meanwhile, if $\tau > d_{\min}/\Delta v$, Q decreases when f increases. The updated information transfer network is related to the new spatial positional relationships among the birds. As a consequence, if $\tau > d_{\min}/\Delta v$, more birds will perceive the external information at the same time as the information transfer network is updated. For the stable information transfer network, $f = 0$; and for the unstable information transfer network, $f = 1/\Delta t$.

V. DISCUSSION AND CONCLUSIONS

To summarize, our information transfer network model depicts how bird flocks perceive and respond to the external stimuli. Based on this information transfer network, we consider another type of interaction among individuals by suggesting that an individual does not always interact with its nearest neighbors and instead interacts with a fixed set of birds in a limited time.

Previously, researchers believed that animals are influenced by neighbors within a certain distance. Recently, researchers have claimed that the interactions between birds in a flock depend on topological distance, rather than metric distance [10, 32]. The neighborhood of each bird is still governed by distance, and there is usually a fixed number of nearest neighbors [31]. Particle-based approaches [29, 31, 41, 42] have been proposed to describe the mechanical dynamics of individuals. In our case, the neighborhood of each bird is static; birds therefore mainly communicate with a fixed set of birds in their neighborhood. Combined with a self-propelled model of birds in a flock, we explore the properties of their movement with a stable information transfer network and compare the performance with an unstable network. Although our hypothesis that the neighbors of each bird are not always the nearest birds is different from that of Ref. [32], our

experiment results indicate that using a stable information transfer network is more robust and closer to both the statistical results generated from empirical datasets [36, 37] and the empirical observations (see Supplemental Material Movies S3-S4 [40]). Therefore, our method with the stable information transfer network can be treated as an improved model to describe the information transfer mechanism of bird flocks.

Our method can be applied to bird flocks. According to Ref. [32], “each bird interacts on average with a fixed number of neighbors (six to seven), rather than with all neighbors within a fixed metric distance.” In our approach, in our method, the bird won’t fly too far away from its neighbors due to the attractions among them. As a consequence, a bird is capable of identifying and tracking six neighbors. Cavagna A et al. [36] find that “the change in the behavioral state of one animal affects and is affected by that of all other animals in the group, no matter how large the group is.” Thus, birds are widely believed to possess the ability to transfer such information in a large murmuration. Birds are social animals and they share their songs to a greater or lesser extent, depending on the degree of their social association [43]. Birds can communicate with each other not only by visual information, but also through verbal cues like song. Therefore, the nearest birds (in terms of Euclidean distance) might not be the ones receiving information transfer because distance is not the sole factor affecting the communications among the birds.

When simulating the information transfer process with a stable network, we find that the information transfer time increases logarithmically with the size of the flock and linearly with the increase in the response time. These results are consistent with the theoretical conclusions drawn from Eq. 4. The number of birds reacting to an external stimulus will affect the total transfer time of the flock, but the effect is negligible. Our method combined with a response time that obeys a Gaussian distribution generates results closer to the empirical datasets because the real response times of birds can vary due to position difference, orientation difference, body conditions, etc.

The previous experiments around bird flocks were based on very short time clips. Therefore, it is currently difficult to verify our model on a large time scale. We need more experimental observations with longer durations and systematic analysis to verify the network with a delayed update. It is worth extending the stable information transfer network to the temporal scenario in which individuals might change their interaction relationships at heterogeneous time scales [44–46] in the future work. In addition to the dynamics of bird flocks, our approach can be applied to other related fields. The stable information transfer network is general and applicable to collective behaviors of other social animals. Our method can also be extended to construct the communication networks of unmanned aerial vehicle groups, robotics, and any other self-organized intelligent agent group.

X.J. was supported by the National Key R&D Pro-

gram of China (Grant no. 2017YFB1002600) and Artificial Intelligence Research Foundation of Baidu Inc. A.L. acknowledges the generous support from the Chair of Systems Design at ETH Zürich, Human Frontier Science Program Postdoctoral Fellowship (Grant: LT000696/2018-C), and Foster Lab at Oxford. D.M. is supported in part by ARO Contract W911NF16-1-0085, and Intel. The authors thank the referee for valuable suggestions.

APPENDIX A: SELF-PROPELLED MODEL

Grouped individuals adjust their velocities according to those of their neighbors and in response to the external stimuli (see Eq. 5). We use mechanical force to represent the factors that drive an individual,

$$\mathbf{F}_{j,i} = \mathbf{F}_{j,i}^{\text{inter}} + \mathbf{F}_{j,i}^{\text{sti}}, \quad (5)$$

where $\mathbf{F}_{j,i}$ is the force working on individual i at frame j , $\mathbf{F}_{j,i}^{\text{inter}}$ is the force in relation to interactions with other birds, and $\mathbf{F}_{j,i}^{\text{sti}}$ is the stimulus force when individual i perceives information about an external stimuli.

The velocity of each individual can be computed according to the following equation,

$$m \frac{\Delta \mathbf{v}_{j,i}}{\Delta t} = \mathbf{F}_{j,i}, \quad (6)$$

where m is the mass of one individual, $\mathbf{v}_{j,i}$ is the velocity of individual i at frame j , and $\Delta \mathbf{v}_{j,i}$ is the difference of $\mathbf{v}_{j,i}$.

Interaction force $\mathbf{F}_{j,i}$ consists of three parts: long-range cohesion $\mathbf{F}_{j,i}^{\text{coh}}$, intermediate-range alignment $\mathbf{F}_{j,i}^{\text{ali}}$ and short-range repulsion $\mathbf{F}_{j,i}^{\text{rep}}$,

$$\mathbf{F}_{j,i}^{\text{inter}} = \mathbf{F}_{j,i}^{\text{coh}} + \mathbf{F}_{j,i}^{\text{ali}} + \mathbf{F}_{j,i}^{\text{rep}}. \quad (7)$$

Cohesion force $\mathbf{F}_{j,i}^{\text{coh}}$ and alignment force $\mathbf{F}_{j,i}^{\text{ali}}$ only occur among agents that are connected to each other, while repulsion force $\mathbf{F}_{j,i}^{\text{rep}}$ occurs among agents within a certain distance and contributes to collision avoidance. We compute $\mathbf{F}_{j,i}^{\text{inter}}$ from two views: graph view for cohesion force $\mathbf{F}_{j,i}^{\text{coh}}$ and alignment force $\mathbf{F}_{j,i}^{\text{ali}}$ (Fig. 5A), and grid view for repulsion force $\mathbf{F}_{j,i}^{\text{rep}}$ (Fig. 5B).

Graph View: In graph view, we treat the flock as an invariant directed graph (Fig. 5A), which represents the stable information transfer network, and use it to compute the attraction force and the alignment force. The borders of zones for repulsion, alignment, and attraction for a given bird are defined by the radii d_r and d_c with $d_c \geq d_r \geq 0$. An individual agent attempts to keep cohesion with its neighbors within the cohesion zone. The cohesion force is defined as

$$\mathbf{F}_{j,i}^{\text{coh}} = \frac{w_{\text{coh}}}{n_{j,i}^{\text{coh}}} \sum_{k \in N_i^{\text{coh}}} \frac{\mathbf{P}_{j,k} - \mathbf{P}_{j,i}}{\|\mathbf{P}_{j,k} - \mathbf{P}_{j,i}\|_2}, \quad (8)$$

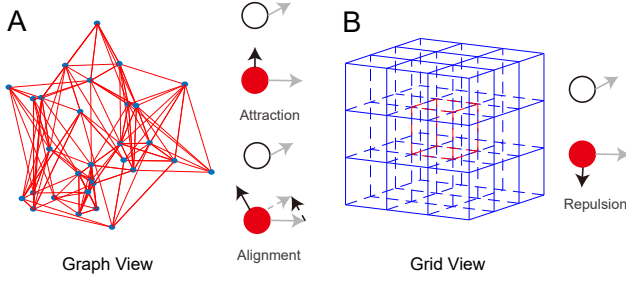


FIG. 5. Graph view and grid view. The red nodes refer to the birds on which we focus, the white nodes refer to the birds around them, the grey arrows refer to the directions of the birds, and the black arrows refer to the directions of the forces. (A) Graph view. The 3D graph represents the stable information transfer network. The blue nodes refer to the birds and the red lines refer to the social relationships between the birds. Attraction and alignment mainly occur between birds that have connections in the graph. (B) Grid view. The 3D grids are segmentations of the 3D space in which the bird flock flies. The red cube represents the minimal sub-grid to which the bird that we focus on belongs. Repulsion occurs among birds in the same or the adjacent minimal sub-grid.

where $\mathbf{P}_{j,k}$ and $\mathbf{P}_{j,i}$ are the positions of bird k and bird i , respectively, and w_{coh} is the weight of $\mathbf{F}_{j,i}^{\text{coh}}$. $N_{j,i}^{\text{coh}} = \{k | k \in N_i, \|\mathbf{P}_{j,i} - \mathbf{P}_{j,k}\|_2 \geq d_c\}$ is the set of neighbors of bird i that are in the scope of cohesion, and $n_{j,i}^{\text{coh}}$ is the number of birds in $N_{j,i}^{\text{coh}}$.

An individual agent attempts to maintain alignment with its neighbors within the zone of alignment. The alignment force is defined as

$$\mathbf{F}_{j,i}^{\text{ali}} = \frac{w_{\text{ali}}}{n_{j,i}^{\text{ali}}} \sum_{k \in N_{j,i}^{\text{ali}}} \frac{\mathbf{v}_{j,k} - \mathbf{v}_{j,i}}{\|\mathbf{v}_{j,k} - \mathbf{v}_{j,i}\|_2} \quad (9)$$

where w_{ali} is the weight of $\mathbf{F}_{j,i}^{\text{ali}}$, $N_{j,i}^{\text{ali}} = \{k | k \in N_i, d_c > \|\mathbf{P}_{j,i} - \mathbf{P}_{j,k}\|_2 \geq d_r\}$ is the set of neighbors of bird i that are in the scope of alignment, and $n_{j,i}^{\text{ali}}$ is the number of birds in $N_{j,i}^{\text{ali}}$.

Grid View: In grid view, we treat the space in which the bird flock flies as a 3D moving grid (Fig. 5B). We use this 3D moving grid to compute the repulsion force.

An individual attempts to maintain repulsion with its neighbors within the zone of repulsion. The repulsion force is defined as

$$\mathbf{F}_{j,i}^{\text{rep}} = \frac{w_{\text{rep}}}{n_{j,i}^{\text{rep}}} \sum_{k \in N_{j,i}^{\text{rep}}} \frac{\mathbf{P}_{j,i} - \mathbf{P}_{j,k}}{\|\mathbf{P}_{j,i} - \mathbf{P}_{j,k}\|_2} \quad (10)$$

where w_{rep} is the weight of $\mathbf{F}_{j,i}^{\text{rep}}$, $N_{j,i}^{\text{rep}} = \{k | \|\mathbf{P}_{j,i} - \mathbf{P}_{j,k}\|_2 \leq d_r\}$ is the set of neighbors of bird i that are in the scope of repulsion, and $n_{j,i}^{\text{rep}}$ is the number of birds in $N_{j,i}^{\text{rep}}$.

In order to efficiently search for the neighbors, we construct a hash table (Fig. 6 C) by splitting the space

around the flock into smaller grids (Fig. 6 A). The center of the 3D grids is the center of the bird flock. The hash table is used to represent proximity information and compute the grid that the bird belongs to. Each data element in the hash table corresponds to a grid in 3D that stores all IDs of birds belonging to that grid. When we compute the repulsion force for one bird, we only need to search the grid to which this bird belongs and the grids that are adjacent to this grid.

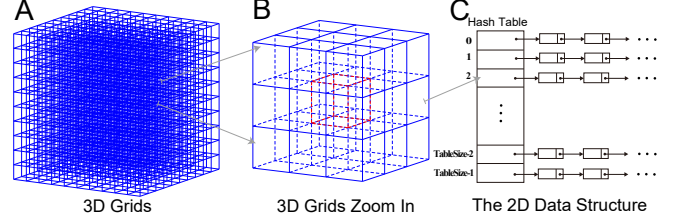


FIG. 6. 3D grids and hash table. (A) 3D grids split the flying space of a bird flock. (B) A zoomed-in version of twenty seven grids. (C) The hash table is the data structure storing the information about the grid to which each bird belongs. The size of the hash table equals the number of the 3D grids. Each element of the hash table corresponds to a grid in (A) storing the IDs of birds that belong to this grid.

Stimulus Force When individuals perceive information about a predator, they try to escape the threat. We define the stimulus force as

$$\mathbf{F}_{j,i}^{\text{sti}} = \frac{\mathbf{P}_{j,i} - \mathbf{P}_j^{\text{pre}}}{\|\mathbf{P}_{j,i} - \mathbf{P}_j^{\text{pre}}\|_2}, \quad (11)$$

where $\mathbf{P}_j^{\text{pre}}$ is the position of the predator at frame j .

Then the stimulus force for attraction would be:

$$\mathbf{F}_{j,i}^{\text{sti}} = \frac{\mathbf{P}_j^{\text{att}} - \mathbf{P}_{j,i}}{\|\mathbf{P}_j^{\text{att}} - \mathbf{P}_{j,i}\|_2}, \quad (12)$$

where $\mathbf{P}_j^{\text{att}}$ is the position of the attraction at frame j .

If there is more than one external stimuli, the stimulus force will be:

$$\mathbf{F}_{j,i}^{\text{sti}} = \frac{1}{N_s} \sum_{k=1}^{N_s} \frac{\mathbf{P}_j^{\chi_k} - \mathbf{P}_{j,i}}{\|\mathbf{P}_j^{\chi_k} - \mathbf{P}_{j,i}\|_2}, \quad (13)$$

where N_s is the number of external stimuli, $\chi_k \in \{\text{pre, att}\}$.

APPENDIX B: SPATIAL CORRELATION

Spatial correlation quantifies the behavior correlation among birds in a certain distance range [36]. The definition of spatial correlation is

$$C(r) = \frac{1}{c_0} \frac{\sum_{ik} \mathbf{u}_i \cdot \mathbf{u}_k \mathbf{H}(r - r_{ik}) \mathbf{H}(r_{ik} - r + 1)}{\sum_{ik} \mathbf{H}(r - r_{ik}) \mathbf{H}(r_{ik} - r + 1)},$$

where r_{ik} is the distance between bird i and j , and c_0 is a normalization factor such that $C(r=0) = 1$. u_i is the fluctuation of bird i around the mean velocity of the flock,

$$\mathbf{u}_i = \mathbf{v}_i - \frac{1}{N} \sum_{k=1}^N \mathbf{v}_k.$$

APPENDIX C: COMPARISON BETWEEN STABLE INFORMATION TRANSFER NETWORK AND UNSTABLE INFORMATION TRANSFER NETWORK

We use the average distance between each bird and the center of the flock D_j to describe the degree of cohesion of the flock at frame j :

$$D_j = \frac{1}{N} \sum_{k=1}^N \left\| \mathbf{P}_{j,k} - \frac{1}{N} \sum_{i=1}^N \mathbf{P}_{j,i} \right\|_2.$$

We compare the cohesion degree between the stable information transfer network and the unstable network, and the results are illustrated in Fig. 7. The flock simulated by our method can maintain cohesion as the time passes, while the flock simulated by the method with unstable information transfer network cannot maintain cohesion and the birds gradually fly become far away from each other (see Supplemental Material Movies S1-S2 [40]).

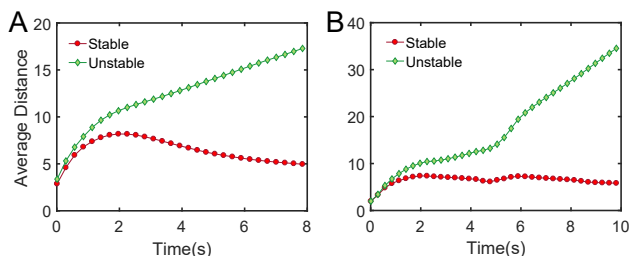


FIG. 7. Cohesion comparison between the stable information transfer network (the red curve) and the unstable one (the green curve). (A) The average distance is plotted versus the time when a fixed external stimulus (predator) attacks the bird flock. (B) The average distance is plotted versus the time when a moving external stimulus (predator) attacks the bird flock.

APPENDIX D: COMPARISON BETWEEN SIMULATION BASED ON OUR METHOD AND EMPIRICAL MOVEMENTS OF BIRDS

We select two clips of empirical movements of bird flocks (from <https://vimeo.com/121168616> and <https://vimeo.com/121168616> respectively). We design the external stimuli according to those videos. The comparison results (shown in Supplemental Material Movies S3-S4 [40]) demonstrate that our method can achieve realistic collective behavior for bird flocks. More simulation results are presented in the Supplemental Material Movies S5-S6 [40].

[1] T. Vicsek and A. Zafeiris, *Phys. Rep.* **517**, 71 (2012).
 [2] H. Shi, G. Xie, M. Yu, and B. Liu, in *Information and Automation (ICIA), 2017 IEEE International Conference on* (IEEE, 2017) pp. 41–46.
 [3] A. Szolnoki and X. Chen, *Phys. Rev. E* **94**, 042311 (2016).

[4] F. L. Pinheiro, F. C. Santos, and J. M. Pacheco, *Phys. Rev. Lett.* **116**, 128702 (2016).
 [5] Y.-Y. Ahn, H. Jeong, N. Masuda, and J. D. Noh, *Phys. Rev. E* **74**, 066113 (2006).
 [6] A. Szolnoki and M. Perc, *New J. Phys.* **20**, 013031 (2018).
 [7] A. Sokolov, I. S. Aranson, J. O. Kessler, and R. E. Goldstein, *Phys. Rev. Lett.* **98**, 158102 (2007).

- [8] D. H. Kelley and N. T. Ouellette, *Sci. Rep.* **3** (2013).
- [9] K. Tunström, Y. Katz, C. C. Ioannou, C. Huepe, M. J. Lutz, and I. D. Couzin, *PLOS Comput. Biol.* **9**, e1002915 (2013).
- [10] W. Bialek, A. Cavagna, I. Giardina, T. Mora, E. Silvestri, M. Viale, and A. M. Walczak, *Proc. Natl. Acad. Sci. U. S. A.* **109**, 4786 (2012).
- [11] M. Moussaïd, D. Helbing, and G. Theraulaz, *Proc. Natl. Acad. Sci. U. S. A.* **108**, 6884 (2011).
- [12] A. Limdi, A. Pérez-Escudero, A. Li, and J. Gore, *Nat. Commun.* **9**, 2969 (2018).
- [13] A. Li, L. Zhou, Q. Su, S. P. Cornelius, Y.-Y. Liu, and L. Wang, arXiv preprint arXiv:1609.07569 (2016).
- [14] J.-L. Deneubourg and S. Goss, *Ethol. Ecol. Evol.* **1**, 295 (1989).
- [15] I. D. Couzin and J. Krause, *Advan. Study Behav.* **32**, 1 (2003).
- [16] M. Gosak, R. Markovič, J. Dolenšek, M. S. Rupnik, M. Marhl, A. Stožer, and M. Perc, *Phys. Life Rev.* (2017).
- [17] T. Walker, D. Sesko, and C. Wieman, *Phys. Rev. Lett.* **64**, 408 (1990).
- [18] H. Ohtsuki, C. Hauert, E. Lieberman, and M. A. Nowak, *Nature* **441**, 502 (2006).
- [19] A. Li, B. Wu, and L. Wang, *Sci. Rep.* **4**, 5536 (2014).
- [20] C. W. Reynolds, *SIGGRAPH Comput. Graph.* **21**, 25 (1987).
- [21] A. Kirman, *Q. J. Econ.* **108**, 137 (1993).
- [22] R. Olfati-Saber, *IEEE Trans. Autom. Control* **51**, 401 (2006).
- [23] H. Blumer, *Soc. Probl.* **18**, 298 (1971).
- [24] J. Qin, Y. Chen, W. Fu, Y. Kang, and M. Perc, *IEEE Access* **6**, 5003 (2018).
- [25] J. K. Parrish and L. Edelstein-Keshet, *Science* **284**, 99 (1999).
- [26] S. L. Lima, *Wilson Bull.* , 1 (1993).
- [27] T. Seeley and R. Morse, *Insectes Soc.* **23**, 495 (1976).
- [28] Y. Wu, A. D. Kaiser, Y. Jiang, and M. S. Alber, *Proc. Natl. Acad. Sci. U. S. A.* **106**, 1222 (2009).
- [29] T. Vicsek, A. Czirók, E. Ben-Jacob, I. Cohen, and O. Shochet, *Phys. Rev. Lett.* **75**, 1226 (1995).
- [30] A. Jadbabaie, J. Lin, and A. S. Morse, *IEEE Trans. Autom. Control* **48**, 988 (2003).
- [31] D. J. Pearce, A. M. Miller, G. Rowlands, and M. S. Turner, *Proc. Natl. Acad. Sci. U. S. A.* **111**, 10422 (2014).
- [32] M. Ballerini, N. Cabibbo, R. Candelier, A. Cavagna, E. Cisbani, I. Giardina, V. Lecomte, A. Orlandi, G. Parisi, A. Procaccini, *et al.*, *Proc. Natl. Acad. Sci. U. S. A.* **105**, 1232 (2008).
- [33] B. Zhou, X. Tang, and X. Wang, in *Comput. Vis. ECCV* (Springer, 2012) pp. 857–871.
- [34] T. Mora, A. M. Walczak, L. Del Castello, F. Ginelli, S. Melillo, L. Parisi, M. Viale, A. Cavagna, and I. Giardina, *Nat. Phys.* **12**, 1153 (2016).
- [35] K. P. Eswaran and R. E. Tarjan, *SIAM J. Comput.* **5**, 653 (1976).
- [36] A. Cavagna, A. Cimorelli, I. Giardina, G. Parisi, R. Santagati, F. Stefanini, and M. Viale, *Proc. Natl. Acad. Sci. U. S. A.* **107**, 11865 (2010).
- [37] A. Attanasi, A. Cavagna, L. Del Castello, I. Giardina, T. S. Grigera, A. Jelić, S. Melillo, L. Parisi, O. Pohl, E. Shen, *et al.*, *Nat. Phys.* **10**, 691 (2014).
- [38] R. Lukeman, Y.-X. Li, and L. Edelstein-Keshet, *Proc. Natl. Acad. Sci. U. S. A.* **107**, 12576 (2010).
- [39] I. D. Couzin, J. Krause, N. R. Franks, and S. A. Levin, *Nature* **433**, 513 (2005).
- [40] See Supplemental Material at [URL] for movies of comparisons and other simulation results.
- [41] J. Ren, X. Wang, X. Jin, and D. Manocha, *PLoS One* **11**, e0155698 (2016).
- [42] D. J. Pearce and M. S. Turner, *J. Royal Soc. Interface* **12**, 20150520 (2015).
- [43] M. Hausberger, M.-A. Richard-Yris, L. Henry, L. Lepage, and I. Schmidt, *J. Comp. Psychol.* **109**, 222 (1995).
- [44] A. Li, S. P. Cornelius, Y.-Y. Liu, L. Wang, and A.-L. Barabási, *Science* **358**, 1042 (2017).
- [45] P. Holme and J. Saramäki, *Phys. Rep.* **519**, 97 (2012).
- [46] R. Olfati-Saber and R. M. Murray, *IEEE Trans. Autom. Control* **49**, 1520 (2004).